95/133

IC/94/385

INTERNATIONAL CENTRE FOR THEORETICAL PHYSICS

THE EFFECT OF GEOMETRIC SCATTERING ON THE OSCILLATORY MAGNETOCONDUCTANCE IN MULTIPLY CONNECTED DISORDERED MESOSCOPIC RINGS

Chaitali Basu

and

Ben–Yuan Gu

INTERNATIONAL ATOMIC ENERGY AGENCY

UNITED NATIONS EDUCATIONAL, SCIENTIFIC AND CULTURAL ORGANIZATION

MIRAMARE-TRIESTE

IC/94/385

International Atomic Energy Agency
and
United Nations Educational Scientific and Cultural Organization
INTERNATIONAL CENTRE FOR THEORETICAL PHYSICS

THE EFFECT OF GEOMETRIC SCATTERING ON THE OSCILLATORY MAGNETOCONDUCTANCE IN MULTIPLY CONNECTED DISORDERED MESOSCOPIC RINGS

Chaitali Basu[1] and Ben-Yuan Gu[2]
International Centre for Theoretical Physics, Trieste. Italy.

MIRAMARE - TRIESTE
December 1994

[1]E-mail: chaitali@ictp.trieste.it
[2]On leave of absence from: Institute of Physics, Academia Sinica, P.O. Box 603, Beijing 100080, People's Republic of China. E-mail: guby@aphy01.iphy.ac.cn

ABSTRACT

We present the quantum mechanical calculations on the conductance of a quantum waveguide consisting of multiply connected mesoscopic rings with disordered ring-circumferences and ballistic lead connections between the rings with the transfer matrix approach. The profiles of the conductance as functions of the magnetic flux and of the Fermi wave number of electrons depend on the number of rings as also on the geometric configuration of the system. The conductance spectrum of this system for disordered ring circumferences, disordered ring intervals and disordered magnetic flux is examined in detail. Studying the effect of geometric scattering and the two different length scales involved in the network, namely, the ring circumference and the ballistic lead connections on the conductance profile, we find that there exist two kinds of mini-bands, one originating from the bound states of the rings, i.e. the intrinsic mini-bands, and the other associated with the connecting leads between the adjacent rings, which are the extra mini-bands. These two kinds of mini-bands respond differently to external perturbations in parameters. Unlike the system of potential scatterers, this system of geometric scatterers show complete band formations at all energies even for finite systems and there is a preferential decay of the energy states depending upon the type of disorder introduced. The conductance band structures strongly depend on the geometric configuration of the network and so by controlling the geometric parameters, the conductance band structures can be artificially tailored.

I. INTRODUCTION

Advances in fabrication technology has furthered the interest in theoretical and experimental investigation of electronic and magnetic properties of mesoscopic systems and nano-structures such as narrow quasi one-dimensional quantum wires, grids, rings, dots, crosses etc[1,2]. These systems are of typically *nm* sizes and ballistic transport of electrons through them is similar to the microwave propagation in waveguides. Hence the general name quantum waveguides[3] is used for those devices where quantum coherence along the whole sample reveals many novel phenomena such as the quantized conductance in point contacts[4], anomalous magnetoresistance in lateral superlattices[5], Hall-Resistance quenching in narrow crosses[6], persistent currents in metallic loops, universal conductance fluctuations, nonlocal current–voltage relations, violations of Onsager relationships, Coulomb blockade in micro-tunnels and several others[7–9]. These systems can be modelled as phase–coherent elastic scatterers and the use of quantum interference as the mechanism for switching action can possibly make devices which are faster and far more economical in energy than the conventional ones, with the functions of an entire circuit being performed by a single element[10–12]. However these quantum devices would not be very robust, as the operational characteristics depend sensitively on material parameters, with control and reproducibility of operating thresholds becoming extremely non-trivial.

Investigations targeted on quantum oscillations and the Aharonov-Bohm effect in a single mesoscopic ring has been of interest for several years now[8,9]. Multiply connected rings with finite quantum wire separation between them has also become a subject of considerable interest[13,14] because at low temperature, the phase coherence length L_ϕ of electron increases significantly. When L_ϕ is comparable to the system size, quantum interference effects become extremely important. A network of many rings much larger than the coherence length L_ϕ has been studied experimentally[15]. So the effect of quantum interference in a system of multiply connected rings working in the ballistic regime may be very interesting to investigate both theoretically[13,14] and experimentally[15], for designing of switching devices based on controlling the relative phase between different interfering paths by applying electrostatic or magnetic fields[10].

In this paper we carry out a detailed investigation on the dependence of conductance of the electron and the Fermi wave–number in multiply connected rings with the use of transfer matrix method[16]. Here we make the circumference of the rings and the length of the inter–connecting ballistic leads disordered, to resemble the experimental situations more closely and investigate the effect disorder in the two different length scales have on the quantum conductance of such systems. We further make the magnetic flux threading the loops disordered and study the magnetoconductance. The motivation to study disorder is to look at the effect that geometric scattering and the dual periodicities may have on the conductance profile, and to compare such a system with the much studied one-dimensional system of potential scatterers.

II. MODEL, THEORETICAL TREATMENT AND FORMULAS

A representative schematic of the serially connected rings is illustrated in Fig. 1. It consists of N rings with different circumferences l_j and different lengths of the inter–connecting quantum leads d_j between the adjacent rings as well as different magnetic fluxes Φ_j threading the rings. The system has thus $2N$ junctions or nodes with each ring having 2 nodes. This structure is further assumed to be connected to two perfectly conducting semi–infinite leads attached at junctions 1 and 2N. When a potential difference is applied across the sample, the two perfect leads serve as the emitter and collector of electrons. We reduce our problem to that of a single electron moving in a one–dimensional quantum wire network, which corresponds experimentally to a network of high–mobility quantum wires with narrow width such that only the lower subband is populated. The left–node coordinates of the

rings are designated by x_j ($j = 1, 2, 3, ...N$) and the distances between adjacent rings, $d_j = x_{j+1} - x_j - l_j/\pi$ ($j = 1, 2, 3, ...N-1$), are allowed to be different. The magnetic flux Φ_j threading the $j-$th ring is completely confined to the interior of the loop. The basic building unit of this quantum wire network is a single ring. We first derive its transfer matrix which relates the wave function coefficients of the electron on one side of the ring to those on the other side (i.e. across the nodes). The global transfer matrix that represents the electron wave propagation through the entire device can then be obtained by cascading all the individual transfer matrices in sequence. We have to use the Griffith quasi-boundary conditions at each node owing to the requirement of the single valuedness of wave functions and the conservation of the current density (Kirchoff law).[3,15,16] For example, at the junction x_j we have

$$\psi_1(x_j) = \psi_2(x_j) = \psi_3(x_j) \tag{1a}$$

and

$$\sum_{i=1}^{3} \frac{d\psi_i}{dx} \mid_{x_j} = 0, \tag{1b}$$

where ψ_1, ψ_2, and ψ_3 represent the electron wave functions of the left-side lead, the upper arm of the ring and the lower arm of the ring respectively. All the derivatives are either outwards or inwards from the junction. In the approximation of single electron, consider an electron with wave number k and the energy $\epsilon(k) = \hbar^2 k^2/2m^*$ propagating through the $j-$th ring. In the presence of the magnetic field the wave function in the ring wire can be expressed as[3]

$$\psi_1 = a_1 e^{ik(x-x_j)} + a_2 e^{-ik(x-x_j)}, \tag{2a}$$

for the left lead of the ring,

$$\psi_2 = c_1 e^{ik_1 s} + c_2 e^{-ik_2 s}, \tag{2b}$$

for the upper arm of the ring,

$$\psi_3 = d_1 e^{ik_2 s} + d_2 e^{-ik_1 s}, \tag{2c}$$

for the lower arm of the ring,

$$\psi_4 = g_1 e^{ik(x-x'_j)} + g_2 e^{-ik(x-x'_j)}, \tag{2d}$$

for the right lead of the ring, where $x'_j = x_j + l_j/\pi$ is the coordinate of the right side node of the $j-$th ring and s is the local coordinate used for the ring. In a one-dimensional ring penetrated by a magnetic flux, one can choose a gauge for which the flux causes only a change in the phase of the wavefunction. Here we have used symmetric gauge for the vector potential of the magnetic field $\mathbf{B_j}$, i.e. $A_j = \Phi_j/l_j$, $\Phi_j = BS_j$ is the magnetic flux through the $j-$th ring of area S_j, and l_j is the circumference of the $j-$th ring. k_1 and k_2 are related to k by

$$k_1 = k + \frac{e\Phi_j}{\hbar c l_j} = k + \frac{\theta_j}{l_j},$$

$$k_2 = k - \frac{e\Phi_j}{\hbar c l_j} = k - \frac{\theta_j}{l_j},$$

and

$$\theta_j = \frac{2\pi\Phi_j}{\Phi_0}, \quad \Phi_0 = \frac{hc}{e}.$$

Φ_0 is the quantum magnetic flux. We have introduced a local coordinate system for each lead such that the direction is along the electron current direction and the origin is taken at the left node of the network for the loops. Using the Griffith quasi-boundary conditions at the left side node of the ring, we have

$$a_1 + a_2 = c_1 + c_2 = d_1 + d_2,$$

$$k(a_1 - a_2) = k_1 c_1 - k_2 c_2 + k_2 d_1 - k_1 d_2. \tag{3}$$

Similarly, at the right side node of the ring,

$$c_1 e^{ik_1 l_j/2} + c_2 e^{-ik_2 l_j/2} = d_1 e^{ik_2 l_j/2} + d_2 e^{-ik_1 l_j/2} = g_1 + g_2,$$

$$k_1 c_1 e^{ik_1 l_j/2} - k_2 c_2 e^{-ik_2 l_j/2} + k_2 d_1 e^{ik_2 l_j/2} - k_1 d_2 e^{-ik_1 l_j/2} = k(g_1 - g_2). \tag{4}$$

From these equations and through the standard algebraic manipulations we can find the relation between the coefficients of the right–side wave function $\{g_1 e^{-ikx'_j}, g_2 e^{ikx'_j}\}$ and those of the left–side wavefunction, $\{a_1 e^{-ikx_j}, a_2 e^{ikx_j}\}$, using the transfer matrix as follows:

$$\begin{pmatrix} g_1 e^{-ikx'_j} \\ g_2 e^{ikx'_j} \end{pmatrix} = M(kx_j) \begin{pmatrix} a_1 e^{-ikx_j} \\ a_2 e^{ikx_j} \end{pmatrix}$$

where

$$M(kx_j) = U^{-1}(ik(x_i + l_j/\pi))m(kl_j)U(ikx_j),$$

$$m(kl_i) = \frac{1}{2Q} \begin{pmatrix} Q^2 - (P-1)^2 & Q^2 - (P^2-1) \\ -[Q^2 - (P^2-1)] & -Q^2 + (P+1)^2 \end{pmatrix}, \tag{5}$$

where

$$P = i2\cos(kl_j/2)/\sin(kl_j/2), \;\; Q = i2\cos(\theta_j/2)/\sin(kl_j/2),$$

$$U(\eta) = \begin{pmatrix} e^{\eta} & 0 \\ 0 & e^{-\eta} \end{pmatrix}.$$

The global transfer matrix can then be constructed as the product of the individual transfer matrices associated with each junction in order. Thus we obtain

$$M_{tot} = U^{-1}(ik(x_N + l_n/\pi))m(kl_N)[\Pi_{j=1}^{N-1} U(ik(x_{j+1} - x_j - l_j/\pi))m(kl_j)]U(ikx_1). \tag{6}$$

The transmission amplitude of the electrons is related to the element of M_{tot} as $t(k) = 1/M_{tot}(2,2)$. For a given configuration of a network of rings, we carry out the matrix multiplication. The two–terminal dimensionless conductance g of the device at small voltages can be written using Landauer's formula,[17,18] as

$$g = G/(\frac{2e^2}{h}) = \mid t \mid^2 . \tag{7}$$

III. NUMERICAL RESULTS AND ANALYSIS

A. Variation of the magnetoconductance profile of serially connected rings – symmetric and asymmetric

Figs. 2 and 3 give the magnetoconductance of an ordered system of serially connected rings (*i.e.* l_j =1, d_j =1, in units of l_0, where l_0 is a scaling length) with increasing number of rings. In Fig. 2(a) at a Fermi wave–number of 0.6π, we plot the magnetoconductance for the system of 1 ring (curve *a*), 3 rings (curve *b*), 8 rings (curve *c*), 14 rings (curve *d*), and 24 rings (curve *e*). As can be seen from the curves with increasing number of rings, the regions of zero transmittance broaden to form a band in the $g-\theta$ spectrum while several new peaks appear in the oscillatory region. These extra oscillatory peaks increase in number with increasing number of rings. In Fig. 2(b) we show the effect of changing Fermi energy on the magnetoconductance of a system of 14 rings. With increase in wavenumber from $kl_0 = 0.2\pi$ to $kl_0 = 0.6\pi$, the highly oscillatory magnetoconductance band increases over a range of θ values. With a further increase in the Fermi wavenumber (and hence energy) to $kl_0 = 1.0\pi$, the conducting band breaks into two sub-bands. Ref. [13] states that θ variation of conductance for single ring system and multiple ring system would be the same. But the above observation contradicts their belief. This is perhaps because of the extra scattering at the several nodes of the multi–ring system and also the effect of the standing wave formation in the ballistic leads that connect rings together. The curves have been given a vertical shift and plotted together for better comparison.

In Fig. 3(a) we study a system of 2 rings in greater details to find out the effect that an increasing circumference would have on the magnetoconductance of a multi–ring system. For all cases we take the length of the ballistic leads equal ($d_j = 1$). We measure all lengths in units of l_0 and so all lengths expressed here are dimensionless. For curve *a*, $l_j = 1$ and for curve *b*, $l_j = 2.5$. As seen the magneto-

conductance oscillates with a larger amplitude for a system of smaller rings while the transmission zeros in the larger ring system outnumber those of the smaller rings. This observation confirms the experimental observation of Umbach *et.al.*[15] that with increase in ring circumference the oscillations decrease exponentially. But from our work we cannot predict the exponential nature of the decay. We now introduce asymmetry into this system. Curve c shows the conductance for the system with $l_1 = 1.0$ and $l_2 = 0.4$ and curve d shows the same for $l_1 = 2.5$ and $l_2 = 1.0$. The ratio l_2/l_1 is kept at 0.4 for both cases. The oscillation decreases for an asymmetric system as compared with a symmetric one (compare curves a with c and b with d) with a definite lowering of the conductance maxima from 1.0. The regions of zero transmittance also narrows with asymmetry. This is perhaps because in an asymmetric system the broken symmetry causes incompleteness of the constructive interference of the wavefunctions. However the effect of asymmetry needs further investigation. Curves c and d are shifted vertically for clarity. In Fig. 3(b), we study this in a system of 3 rings. In curve a, $l_1 = l_2 = l_3 = 1$ (*i.e.* an ordered system), curve b has $l_1 = l_3 = 1.0$ and $l_2 = 1.5$ while curve c has $l_2 = 1.9$. With increase in circumference of the middle ring, the conductance peaks around $\theta = 2.0\pi$ move nearer each other with an increase in the zero conductance region. Curve d shows a system with $l_1 = l_3 = 1.5$ and $l_2 = 1.0$. This curve is exactly the same as that of the ordered system (curve a). Curves $b - d$ are shifted vertically for better comparison.

We now look at the zero field case and study the effect of changing Fermi–energy on the conductance profile of the multi–ring system. In Fig. 4(a), we plot g vs kl_0/π for 1-4 rings in curves $a - d$ respectively. For a single ring, the conductance oscillates periodically with kl_0/π and the peaks are associated with the quasi–bound states within the ring. We refer to these peaks as the intrinsic conductance band. In curve b, for two rings separated with a finite ballistic lead, we observe the appearance of extra peaks at the conductance valleys of the single ring

system. Then with increase in the number of rings in the system, this extra peak splits to give $N - 1$ peaks (N is the number of rings). This is similar to the case of periodic potential scatterers which gives $N - 1$ resonances in an allowed band. But for the periodic potential scatterers, presence of so few scatterers would have never produced the entire band structure. The conductance peaks belonging to the single ring develop into the flatter conductance plateaus which we refer as the intrinsic conductance bands. The extra conductance band with highly oscillatory structures are originated from the ballistic lead separation of the rings, referred henceforth as the extra conductance band. These two kinds of conductance bands have essentially different characteristics and behaviors in response to the external perturbation (see next section). In Fig. 4(b) we study the magnetoconductance of a system of 5 rings. Curve a shows the zero field case. As seen there are the extra conductance bands with 4 (*i.e.* $N - 1$) peaks in the extra conductance bands and the flat transmitting regions with small oscillatory ripples of the intrinsic conductance bands. With increase in flux from $\theta = \pi^2/8$ in curve b to $\theta = 0.5\pi$ in curve c, owing to the presence of the magnetic flux through each loop, each of the intrinsic bands split into two (except the lowest one) and a band gap is formed at some energies within the original intrinsic band. This is because the magnetic field breaks the time–reversal symmetry with the degeneracy of the original two-fold degenerate eigenstate of the ring being lifted. This causes the intrinsic conductance peaks to split into two peaks with a zero in the transmission developing in-between to form a new gap. However, the extra conductance bands associated with the connection leads between the adjacent rings remain unchanged in their energy location with only a decrease of the oscillation amplitude. On applying a large magnetic flux, (as seen in curve c) the split peaks move apart with an increase in the new band gap. With increase in magnetic flux, these peaks tend to merge with the neighboring extra conductance band. The width of this new band-gap increases with increase in magnetic flux. Curves b and c have been

shifted vertically for clarity.

In Fig. 5 we look into the effect of changing the ballistic lead lengths on the nature of the band structures. For a system of 10 rings, we plot g vs kl_0/π for $d_j = 0$ in curve a, $d_j = 1$ in curve b and $d_j = 2$ in curve c. Comparing curves a and b of Figs. 5 we find that the original intrinsic conductance bands substantially split into many sub–bands and a number of extra conductance bands are created in the original band gaps. The number of these splitting sub–bands and the extra conductance bands increases with an increase in the length of the connecting leads. Here we would like to emphasize the fact that the features of these mini–bands are different depending on their origin, belonging to the intrinsic bands or the extra bands. From their response to the external perturbation, one can distinguish them clearly. These results are similar to Ref. [13] where they find a miniband structure each having $N-1$ peaks (when $d_j = 0$) similar to the one–dimensional serially connected superlattices. With introduction of the finite ballistic leads connection, the original miniband structure breaks into smaller minibands while extra conductance bands appear in between. Of these minibands some have flat plateaus with small oscillatory structures belonging to the intrinsic bands while the others have highly oscillatory peaks belonging to the extra conductance bands. With increase in the length of the ballistic leads, the number of minibands increase with the conductance becoming highly oscillatory. Takai and Ohta[13] suggests that the appearance of the extra minibands with introduction of the ballistic leads is because of an increase in the number of nodes and hence an increase in number of potential barriers at which scattering takes place. But this does not account for the increase in number of minibands with an increase in the length of the ballistic leads keeping the number of nodes constant. This strong dependence of conductance on the ballistic leads is also seen in Ref. [14]. These results are expected owing to an increase in the number of harmonics of the standing wave that survive in the ballistic leads with an increase in the length of the leads. The

intrinsic conductance peaks because of the quasi–bound states in the rings and the standing waves in the ballistic leads cause such richly structured conductance profile in this model. Although in multiple double barrier quantum well structures and in multiple quantum wells with impurities doped in the wells, there are quasi–bound state formations, we do not find the appearance of complete extra bands in the conductance profile for so few number of basic building units. The specific quasi–bound states formed in the rings are responsible for the periodic band-gaps to form rapidly even for a few rings, which was absent for the above structures. This is owing to different properties of the basic building units of these systems.

B. Effect of disorder on the oscillatory conductance

In an experimental situation, it is very difficult to make high–precision scaled samples. So the study of the disorder effect on the conductance profile is very important for the working of devices. In the previous section, we have seen the change in the conductance profile due to geometric scattering and the dual periodicities of the circumference and the leads. Here we introduce aperiodicity through disorder in circumference and ballistic leads and then study the decay of conductance with increasing electron energy. We also wish to compare this system of geometric scatterers with the much studied system of potential scatterers. We introduce the disorder in the lengths of ring circumference and the ballistic leads of the multi-ring system. In Fig. 6 we study the effect of the different types of disorder on the conductance profile of a system of 20 rings. Curves have been vertically shifted for clarity. Fig. 6(a) shows the effect of circumference disorder w_c, 6(b) shows that of the lead disorder w_d and 6(c) shows the effect of a disorder in the magnetic flux threading the rings. In all the above cases we plot the ensemble averaged conductance $< g >$ over 1200 configurations vs kl_0/π.

In Fig. 6(a), we calculate the circumferences as

$$l_j = (1 + R_j.w_c)l_0. \qquad (8a)$$

where R_j is a random number with a uniform distribution between -0.5 to +0.5 and l_0 is the basic unit of circumference (=1, taken here). Curves $a-e$ correspond to w_c= 0.0, 0.1, 0.2, 0.3, and 0.4, respectively. With increase in disorder, $< g >$ decreases with the intrinsic band states tending to decay faster than those of the extra bands. The ripples imposed on the intrinsic bands are substantially smeared, in contrast with the oscillatory structures in the extra bands where suppression is much less.

In Fig. 6(b), we calculate the ballistic lead lengths as

$$d_j = (1 + R_j.w_d)d_0. \tag{8b}$$

d_0 is the basic unit of lead length (=1, taken here). Curves $a-f$ correspond to w_d equal to 0.0, 0.1, 0.2, 0.3, 0.4, and 0.5, respectively. With increase in disorder only the extra bands belonging to the finite sized connecting leads decay completely. However, the intrinsic bands do not appear to have the decay behaviour. In particular, the intrinsic conductance peaks associated with the single ring always remain at unit value. This is expected owing to the fact that these intrinsic bands are associated with the quasi–bound states in the rings. They do not show significant response to the perturbation in the length of the connecting leads. The shape of the intrinsic bands are however sharpened. At $w_d = 0.5$, the conductance profile shows sharp resonance peaks.

In Fig. 6(c), we plot $< g >$ vrs kl_0/π for disordered magnetic flux threading the rings. We calculate the magnetic flux as

$$\phi_j = R_j.w_f.f_0. \tag{8c}$$

f_0 is the basic unit of flux (=1, taken here). Curves $a-e$ correspond to w_f = 0.0, 0.1, 0.2, 0.3, and 0.4 respectively. With introduction of the minimum disorder in the magnetic flux, each intrinsic miniband splits into two bands at finite magnetic field because of the breaking of the time–reversal symmetry [14].

In contrast, the energy position and oscillatory nature of the extra minibands essentially remain intact to any magnetic flux fluctuation. The different property of these two kinds of minibands are revealed again. With further increase in disorder the conductance maxima of the split intrinsic bands decrease faster with an overall decrease in $< g >$. The forbidden gap between the split peaks also increases with w_f substantially, smearing out the small oscillations.

It is worth mentioning that the first intrinsic conductance band at zero energy is extremely sensitive to the weak magnetic flux fluctuation. On introducing the magnetic flux perturbation, the conductance value at zero energy abruptly changes from unity to zero owing to the symmetry breaking property of the magnetic field . This transition occurs sharply. On increasing the magnetic flux, this zero transmission point located at the zero energy region broadens to a gap shifting considerably towards the high energy region, as seen in curves $c-e$. This behaviour of the intrinsic band is expected, as the effect of the magnetic field is only in the phase of the electron waves travelling in the different arms of the same ring. So a disorder in magnetic field will have similar effects as a disorder in the circumference. Tuning of the magnetic field shifts the bands on the energy axis – an effect also observed in Ref. [14].

As is seen for both circumference disorder and lead disorder, the electron states with lower values of kl_0 are not much affected. This is because, these electrons have larger wavelengths and the system size is too small for them to feel the effect of breaking periodicity either in the circumferences or leads. But as soon as a finite magnetic field is introduced, the time reversal symmetry is broken, with a transmission zero appearing at the centre of the bands. So all energy states are affected and a conductance minima appears at zero energy. Disorder in the ballistic leads seem to have much slower effect in making all electron states of a multi-ring system non-conducting than a disorder in the loop circumferences or the magnetic fields threading the loops. The difference of the geometric scatterers

from the potential scatterers is also seen in the fact that introduction of slightest disorder in the latter case makes all energy states localised expect for the presence of some stochastic resonances. Whereas for the geometric scatterers, we find that there is a preferential decay of the energy states depending upon the type of disorder introduced. However in both cases for large system (or strong disorder) the states are all exponentially localised. From these results we can find that by controlling and changing the geometric parameters of the system the conductance band structures can be artifically tailored to design new model devices. Also we find that the stability of the two types of minibands depend on the different external perturbations or fluctuations which may be an useful information to guide the design of the devices.

VI. CONCLUSION AND REMARKS

We have presented the magnetoconductance profile study for the quantum multi-ring system connected to ballistic leads for different values of the Fermi wave number of electrons. This model device involves two periodic lengths : ring circumference and connecting lead lengths. We found that miniband structures are formed with increase in the number of rings. There are two types of minibands - one is the intrinsic miniband which are formed due to the presence of quasi-bound states in the rings and the other is the miniband formed by the standing waves in the ballistic leads. These two kinds of minibands bahave differently in response to external perturbations. These characteristics are very different from the one-dimensional potential scatterer system. This is due to the fact that in our model, the multiring geometry gives rise to well defined forbidden and allowed regions. Change in periodicity of one length scale alters only the corresponding mini-bands keeping the others intact. Asymptotically both geometric scatterers and potential scatterers localises all energy states exponentially. However in the mesoscopic regime, for the system of geometric scatteres, disorder in either of the

length scales involved in the system tends to cause a preferential localisation in the energy states. This is never the case for the potential scatterers. By controlling and tuning the geometric parameters of the model devices, the conductance band structures may be artificially tailored to meet the desired performance.

ACKNOWLEDGMENTS

One of the authors (B.Y.G) would like to thank Professor Abdus Salam, the International Atomic Energy Agency and UNESCO for hospitality at the International Centre for Theoretical Physics, Trieste. (C.B) would like to thank the International Centre for Theoretical Physics for the financial assistance as Postdoc during the period of this work.

REFERENCES

[1] L. Pfeiffer, K. W. West, H. L. Stormer, J. P. Eisenstein, K. W. Baldwin, D. Gershoni and J. Spector, , Appl. Phys. Lett. **56**, 1697 (1990)

[2] *The Physics and Fabrication of Microstructure and Microdevices*, edited by M. J. Kelly and C. Weibuch (Springer, Berlin, 1986); *Nanostructure Physics and Fabrication*, edited by M. A. Reed and W. P. Kirk (Academic , New York, 1989); *Physics and Technology of Submicron Structures*, eds. H. Heinrich, G. Bauer and F. Kuchar (Springer, NewYork, 1988)

[3] J. B. Xia, Phys.Rev.B **45**, 3593 (1992)

[4] B. J. van Wees, H. van Houten, C. W. J. Beenakker, J. G. Williamson, L. P. Kouwenhoven, D. van der Marel, and C. T. Foxson, Phys. Rev. Lett. **60**, 848 (1988); B. J. van Wees, L. P. Kouwenhoven, E. M. M. Willems, C. J. P. M. Harmans, J. E. Mooij, H. van Hauten, C. W. J. Beenakker, J. G. Williamson, and C. T. Foxon, Phys. Rev. B **43**, 12 431 (1991); D. A. Wharam, T. J. Thornton, R. Newbury, M. Pepper, and H. Richie and G. A. C. Jones, J. Phys. C **21**, L209 (1988).

[5] See e.g., D. Weiss, in *Electronic Properties of Multilayers and Low Dimensional Semiconductor Structures*, edited by J. M. Chamberlain, L. Eaves and J. C. Portal (Plenum, NewYork, 1990)

[6] M. L. Roukes, A. Scherer, S. J. Allen, H. G. Craighead, R. M. Ruthen, E. D. Beebe and J. P. Harbinson, Phys. Rev. Lett. **59**, 3011 (1987)

[7] *Quantum Coherence in Mesoscopic Systems*, edited by B. Kramer, vol. **254**, *NATO ASI Series B : Physics* (Plenum, NewYork, 1991);*Mesoscopic Phenomenon in Solids*, edited by B. L. Altshuler, P. A. Lee and R. A. Webb (North-Holland, Amsterdam, 1991); C. W. J. Beenakker and H. van Houten, in *Solid State Physics : Semiconductor Heterostructures and Nanostructures*, edited by H. Ehrenreich and D. Turnbull (Academic, NewYork, 1991)

[8] S. Washburn and R. A. Webb, Adv. Phys. **35**, 75 (1986); R. Webb, S. Washburn, C. Umbach and R. Laibowitz, Phys.Rev. Lett. **54** , 2696 (1985); V. Chandrashekhar, M. Rooks, S. Wind and D. Prober, *ibid.* **55**, 1610 (1985); S. Datta, M. Melloch, S. Bandyopadhyay , R. Noren, M. Vaziri, M. Miller anf R. Reifenberger, *ibid.* **55**, 2344 (1985)

[9] Y. Gefen, Y. Imry and M. Azbel, *ibid.* **52**, 129 (1984) ; N. Kumar and A. M. Jayannavar, Phys.Rev.B, **32**, 3345 (1985) ; D. A. Browne, J. P. Carini and S. R. Nagel, Phys. Rev. Lett. **55**, 136 (1985); R. Landauer and M. Buttiker, *ibid.* **54**, 2049 (1985); A. D. Stone and Y. Imry, *ibid.* **56**, 189 (1986)

[10] F. Sols, M. Macucci, V. Ravoili and K. Hess, Appl. Phys. Lett. **54**, 350 (1990); J. Appl. Phys. **66**, 3892 (1989); A. M. Jaynnavar and P. Singha Deo, Mod. Phys. Lett. B **8**, 301 (1994)

[11] R. Landauer, Physics Today **42**, No. 109, 119 (1989)

[12] S. Subramaniam, S. Bandopadhyay and W. Porod, J.Appl.Phys. **68**, 4861 (1990)

[13] D. Takai and K. Ohta, Phys.Rev.B **50**, 2685 (1994)

[14] P. Singha Deo and A. M. Jayannavar, Phys. Rev. B **50**, 11629 (1994)

[15] C. P. Umbach, C. V. Haesendonck, R. B. Laibowitz, S. Washburn and R. A. Webb, Phys. Rev. Lett. **56**, 386 (1986)

[16] B. Y. Gu (unpublished)

[17] R. Landauer, Z. Phys. B **68**, 217 (1987); J. Phys. Condens. Matter **1**, 8099 (1989)

[18] M. Buttiker, Y. Imry, R. Landauer and S. Pinhas, Phys. Rev. B **31**, 6207 (1985)

FIGURE CAPTIONS

FIG. 1 Schematic representation of a multiring system inter-connected by ballistic leads. For a system of N rings there are N-1 interconnecting leads and 2N nodes. The positions of the left nodes are designated by x_j (j=1,2,3... N). The right nodes are determined by $x'_j = x_j + l_j/\pi$. The circumference of the loops are l_j (j=1,2,3...N) and the ballistic leads are denoted by $d_j = x_{j+1} - x_j - l_j/\pi$.

FIG. 2 Magnetoconductance g versus flux per ring θ/π. (a) A system of 1 ring (curve a), 3 rings (curve b), 8 rings (curve c), 14 rings (curve d) and 24 rings (curve e) at $kl_0 = 0.6\pi$ for all seperations $d_j = 1.0$ and loop circumference $l_j = 1.0$. Curves b–e are vertically shifted for clarity, (b)A system of 14 rings at different Fermi wavenumber (and hence energy) of the traversing electron.

FIG. 3 Magnetoconductance g as a function of flux per ring θ/π (a) A system of 2 rings (symmetric – curves a,b and asymmetric – curves c,d) at $kl_0 = 1.0\pi$, where l_0 is a scaling length, for loop circumferences $l_j = 1$ (curve a), $l_j = 2.5$ (curve b), $l_1 = 1.0, l_2 = 0.4$ (curve c) and $l_1 = 2.5, l_2 = 1.0$ (curve d). Curves c and d are vertically shifted for clarity. (b) A system of 3 rings. Curve a is for the symmetric case $l_j = 1.0$, Curve b has $l_1 = l_3 = 1.0$ and $l_2 = 1.5$, Curve c has $l_2 = 1.9$ and Curve d has $l_1 = l_3 = 1.5$ and $l_2 = 1.0$.

FIG. 4 Oscillatory conductance g versus scaled Fermi-wavenumber kl_0/π for various fluxes θ and number of rings N. (a) $\theta = 0.0$ and N $= 1 - 4$, curves (a-d) For all curves $l_j = d_j = 1.0$ (*i.e.* system is ordered) (b) for an ordered system consisting of 5 rings with zero magnetic field (curve a), $\theta = \pi^2/8$ (curve b) and $\theta = 0.5\pi$ (curve c)

FIG. 5 Conductance g as a function of the Fermi wave number kl_0/π, at zero field for a system of 10 rings. Here we study the effect of ballisic lead length d_j on the profile of g. Curve a is for the system with no ballistic leads (*i.e.* $d_j = 0.0$) . As seen it contains only the minibands due to the loops. Curves b and c are for the system with ballistic leads ($d_j = 1, 2$ respectively). As seen with

increase in the lead length, more minibands appear and the profile becomes highly oscillatory.

FIG. 6 The ensemble-averaged value of conductance, $< g >$ plotted as a function of Fermi wave-number kl_0/π for a system of 20 rings at zero field (a) Increasing circumference disorder w_c=0.0, 0.1, 0.2, 0.3, 0.4 (curves $a - e$), (b) Increasing lead disorder w_d = 0.0, 0.1, 0.2, 0.3, 0.4, 0.5 (curves $a - f$). The features to note are the faster decay of some minibands and the lower energy electrons remaining unaffected, (c) Increasing disorder in magnetic flux threading the circumference, w_f=0.0, 0.1, 0.2, 0.3, 0.4 (curves $a - e$). The minibands due to the loops split in two due to breaking to time reversal symmetry (and consequent lifting of the energy degeneracy) and these subbands decay faster than the other minibands. Here the point to observe is that even low energy electrons are affected.

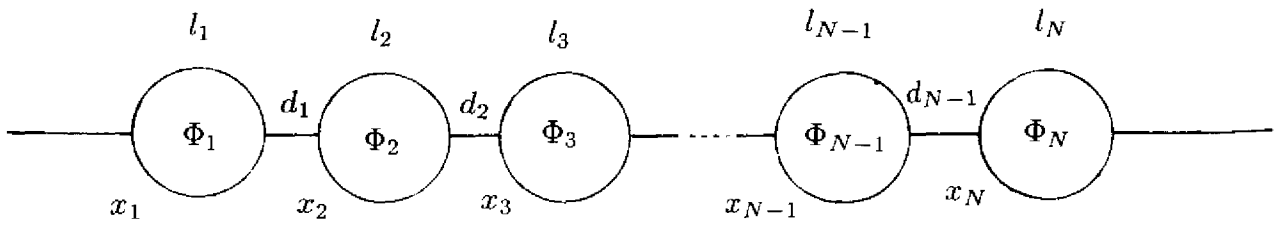
l_1
l_2
l_3
l_{N-1}
l_N
d_1
d_2
d_{N-1}
Φ_1
Φ_2
Φ_3
Φ_{N-1}
Φ_N
x_1
x_2
x_3
x_{N-1}
x_N

Fig. 1

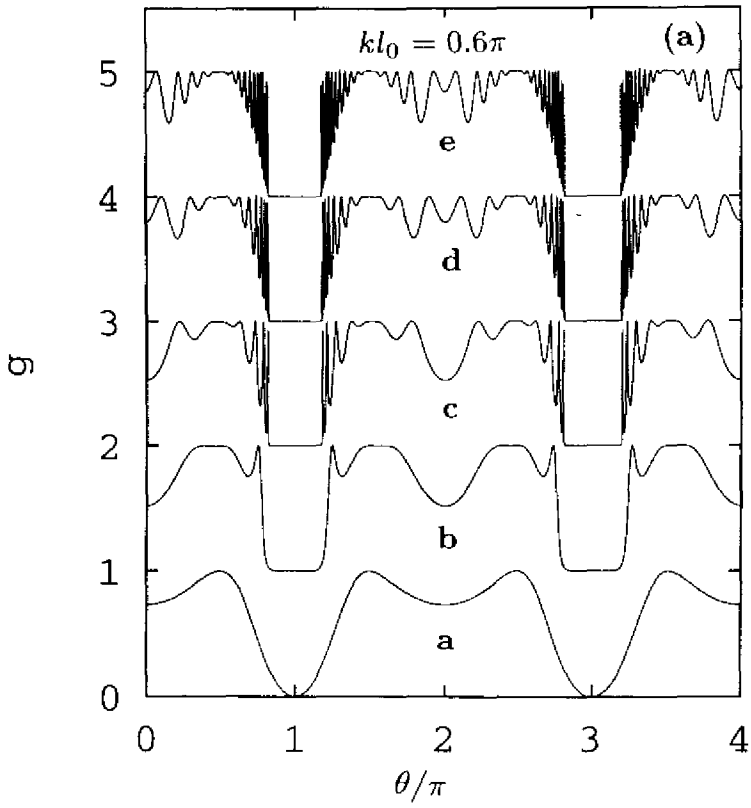
$kl_0 = 0.6\pi$
(a)
e
d
c
b
a
g
0
1
2
3
4
5
θ/π

Fig. 2(a)

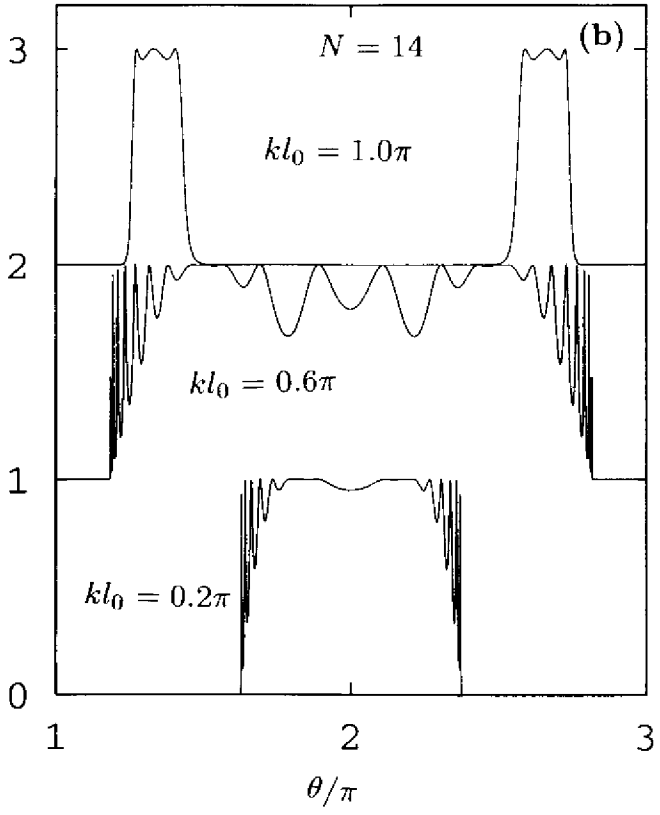
N = 14
(b)
kl0 = 1.0π
kl0 = 0.6π
kl0 = 0.2π
g
θ/π
0
1
2
3

Fig. 2(b)

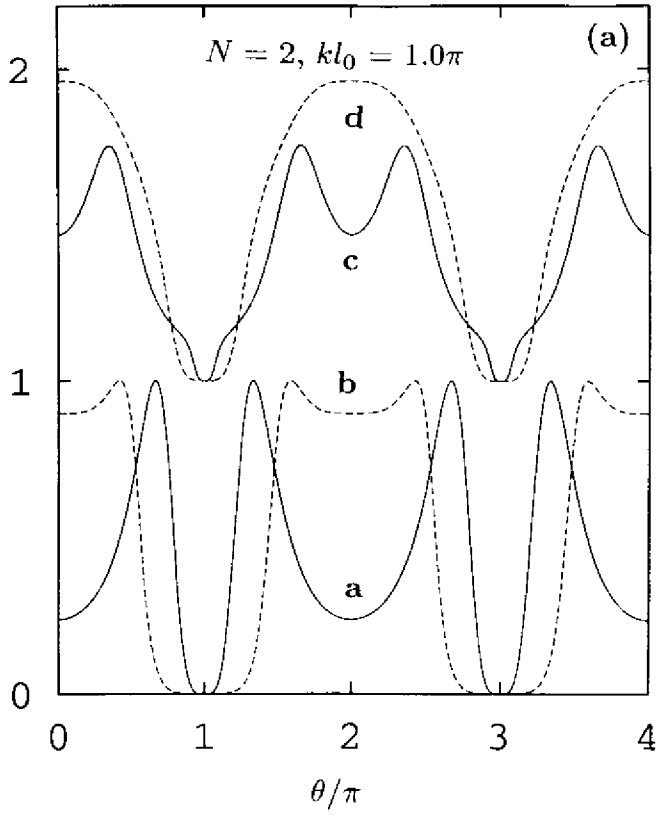
N = 2, kl0 = 1.0π
(a)
d
c
b
a
g
θ/π
0
1
2
3
4

Fig. 3(a)

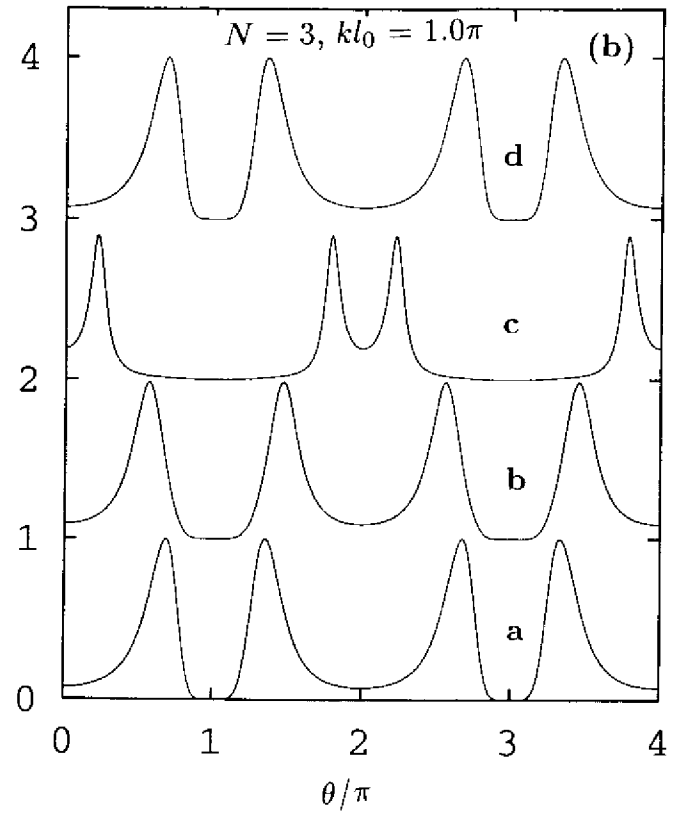
$N = 3,\ kl_0 = 1.0\pi$
(b)
d
c
b
a
g
0
1
2
3
4
θ/π

Fig. 3(b)

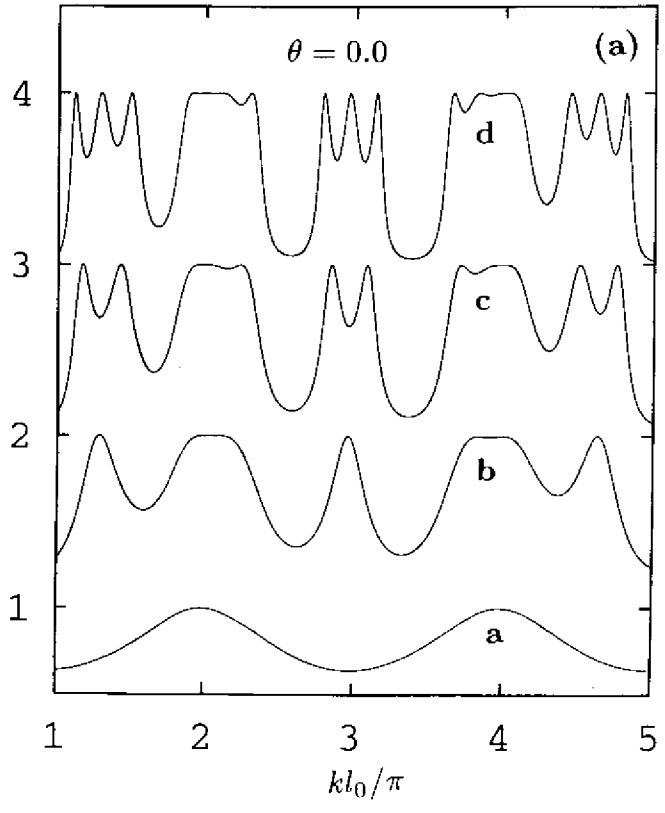
$\theta = 0.0$
(a)
d
c
b
a
g
1
2
3
4
5
kl_0/π

Fig. 4(a)

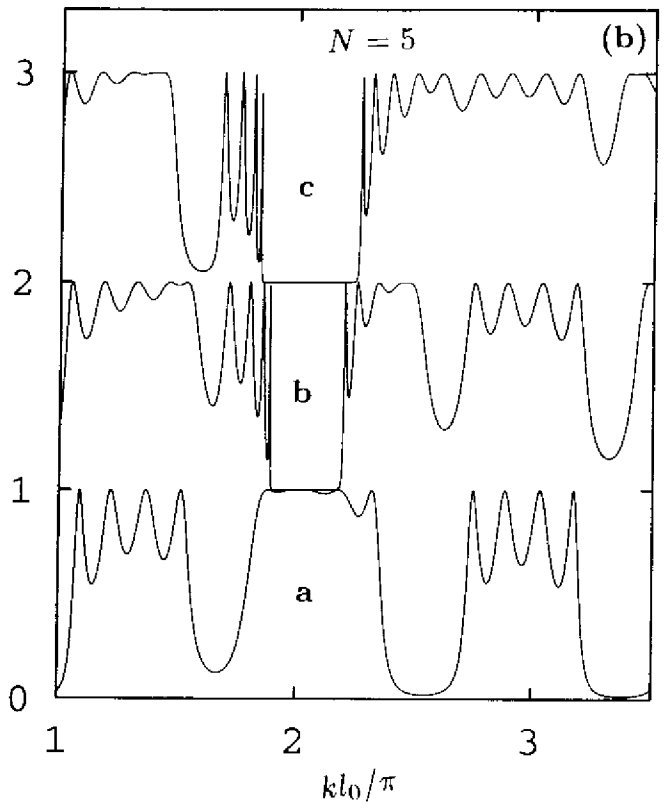

Fig. 4(b)

Fig. 5

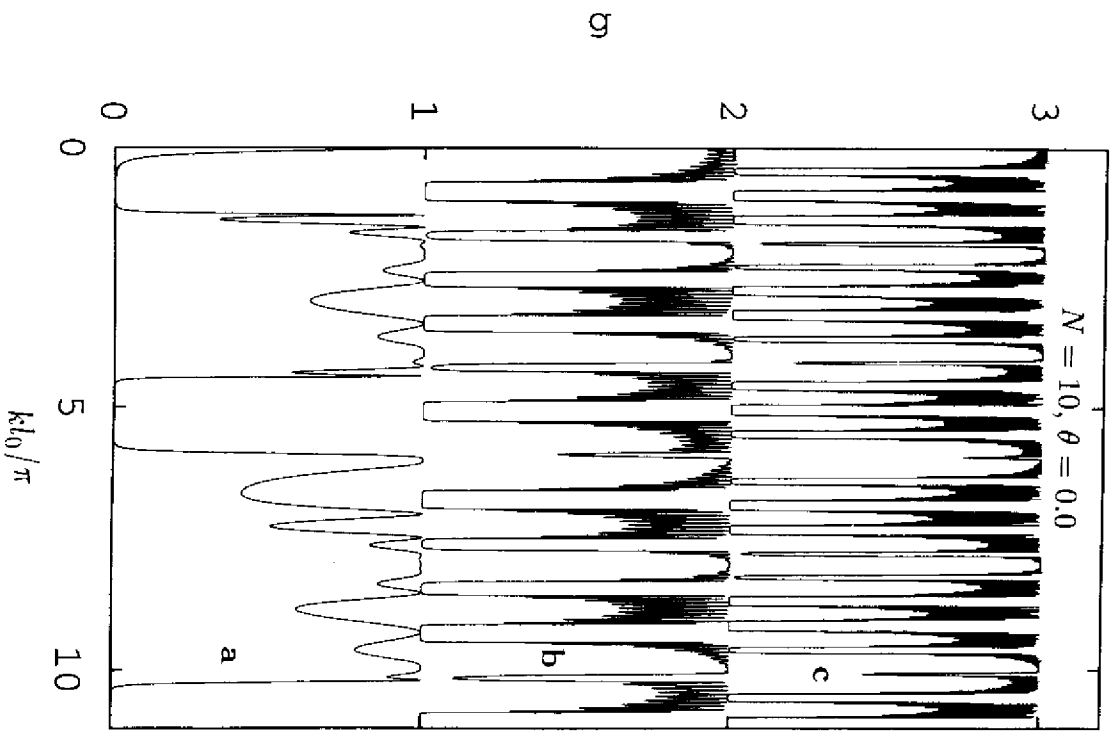

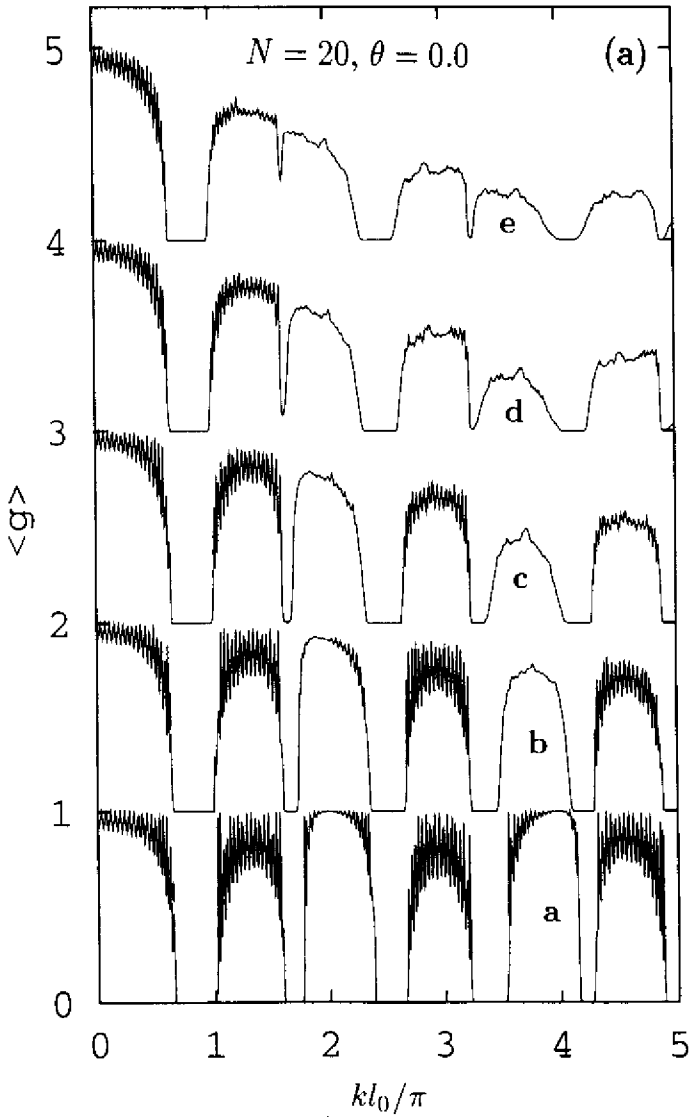

Fig. 6(a)

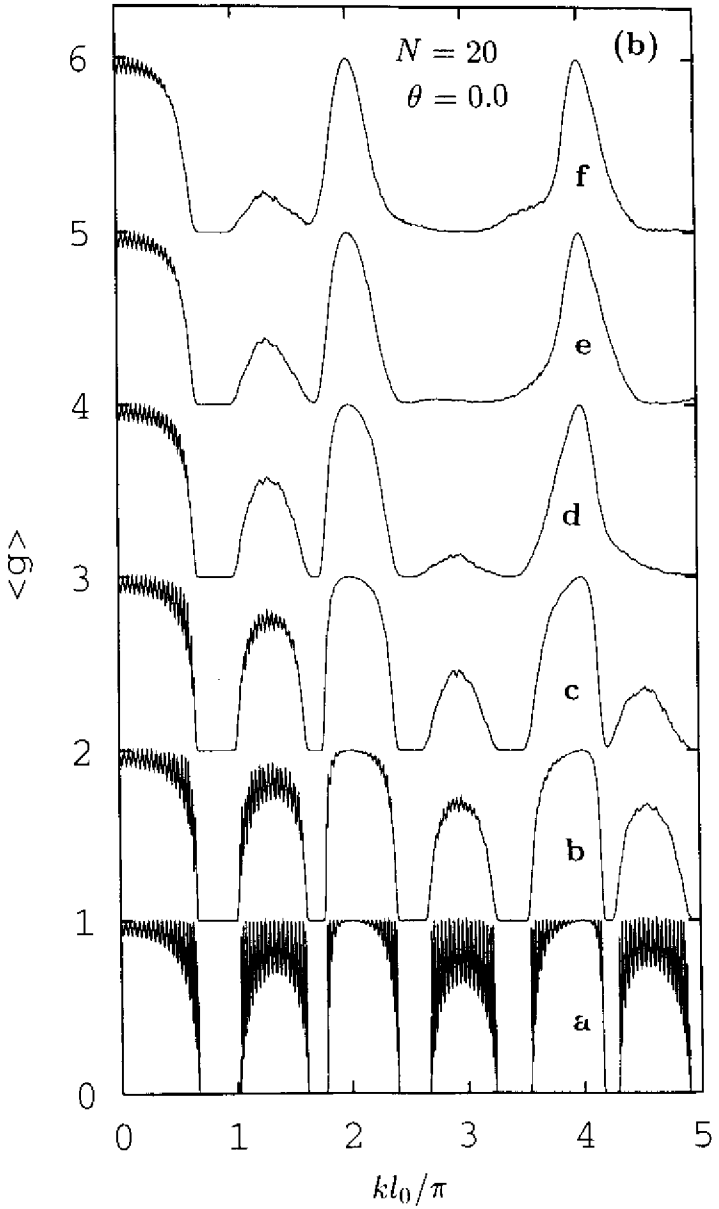

Fig. 6(b)

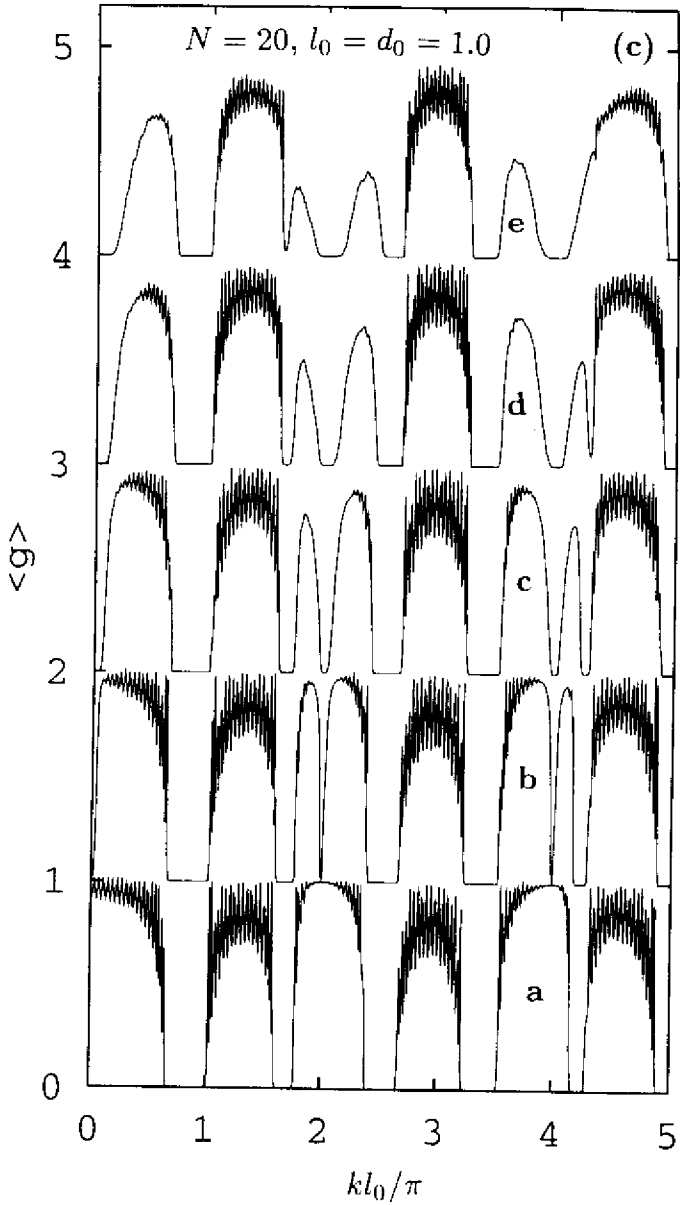

Fig. 6(c)